Strong green upconversion emission from Er^{3+}–Yb^{3+} co-doped $KCaBO_3$ phosphor

Subrata Das, A. Amarnath Reddy, G. Vijaya Prakash *

Nanophotonics Laboratory, Department of Physics, Indian Institute of Technology Delhi, New Delhi 110016, India

A R T I C L E   I N F O

A B S T R A C T

Potassium calcium mixed borate, $KCaBO_3$:Er^{3+}, phosphors with varied Yb^{3+} concentrations were synthesized by solid-state reaction and studied for the first time. The obtained single monoclinic phased polycrystalline phosphor has the capability of accepting the Yb^{3+} sensitizer up to 16 wt.%. Monotonically increasing green upconversion emission ($^2H_{11/2}$,$^4S_{3/2} \rightarrow {}^4I_{15/2}$) of Er^{3+} with the increase of Yb^{3+} concentration is observed under 980 nm laser excitation. Upconversion mechanism is investigated in detail and attributed to the efficient resonant energy transfer from Yb^{3+} to Er^{3+} ions in such system. Our results suggest a potential material for green upconversion phosphor.

© 2011 Elsevier B.V. All rights reserved.

1. Introduction

In the last few decades much attention has been paid to the research on rare-earth doped luminescent materials owing to the application in various technologies, such as high power and coherent laser sources [1], three-dimensional displays [2,3], and bioassays [4]. Realization of solid state RGB (red, green, and blue) light emitters, requires precise control on generation and intensity of emitted light for future high brightness full-color display technology. Among others, special attention has been given to rare-earth doped hosts emitting in the visible range upon infrared excitation (upconversion process (UPC)) [5–7]. Co-doping with Yb^{3+} as sensitizer further increases the efficiency of the UPC process through donor–acceptor processes in rare earths like Tm^{3+}, Ho^{3+}, Er^{3+} ions [8–16]. The combined Er^{3+}/Yb^{3+} doped low phonon energy host matrices [17–23] are of special interest, wherein the UPC results into efficient blue, green, and red emissions. The large spectral overlap between Yb^{3+} emission ($^2F_{5/2} \rightarrow {}^2F_{7/2}$) and Er^{3+} absorption ($^4I_{15/2} \rightarrow {}^4I_{11/2}$) is responsible for such efficient resonant energy transfer (ET) from Yb^{3+} to Er^{3+}.

Inorganic borates have been the focus of optoelectronic research because of their wide range of transparency over a wide spectral range, designer-flexible structure and durable for mechanical and high-laser usages. Recent advances in alkali and alkaline earth mixed borates demonstrated their importance in optoelectronics as red/green phosphors, dosimetric applications based on thermoluminescence and nonlinear optical (NLO) applications [24–26]. While mixed borates are extensively used as red/green phosphors, the synthesis of single phased borates are relatively rare to obtain from solid state reactions. Particularly owing to advances in IR sources, UPC green/red phosphors are of special sub-

ject of interest. In particular co-doping effects on Er^{3+} emission is critically dependent on structure of host matrix, excited state absorption (ESA) and energy transfer (ET) between the f–f transitions of Er^{3+} and/or Er^{3+}/Yb^{3+} combined system. Therefore, systematic research on synthesis mechanism, structure and resultant effects on phosphor characteristics is necessary and worthy of pursuit.

In this Letter the upconversion as well as the downconversion emission properties of $KCaBO_3$ co-doped with Er^{3+} and Yb^{3+} ions is systematically investigated for the first time. We report the synthesis of single monoclinic phase doped $KCaBO_3$ having capability of large concentration of rare earth doping which gives remarkably intense green emission ($^2H_{11/2}$,$^4S_{3/2} \rightarrow {}^4I_{15/2}$) through cooperative upconverted emission on 980 nm excitation. Explanations based on structure, sensitizer dependence, and energy transfer mechanisms are discussed and presented.

2. Experimental details

The potassium calcium mixed borate ($KCaBO_3$) phosphors co-doped with Er^{3+}/Yb^{3+} were synthesized by solid state diffusion method. A mixture containing analytical grade KCl, $CaCl_2$, and H_3BO_3 in stoichiometric ratio with 2.0 wt.% of Er_2O_3 and x.0 wt.% ($x = 0$, 2, 4, 8, 12, and 16) of Yb_2O_3 was ground into fine powder in a mortar. This mixture was heated in air atmosphere up to 450 °C for 1 h and then to 950 °C for 21 h in a silica crucible, then was cooled to room temperature by rapid cooling. X-ray diffraction (XRD) data for all these polycrystalline samples was collected on XPERT-PRO diffractometer with Cu Kα radiation ($\lambda = 1.54$ Å). The cell parameters were estimated from standard expressions and further refined from the simulations of 'EXP2004' software [27]. The steady-state and time-resolved emission measurements were carried using home built setups using 980 nm diode laser (for upconversion) and 532 nm DPSS laser (for downconversion) as excitation

* Corresponding author. Fax: +91 011 2658 1114.
  E-mail address: prakash@physics.iitd.ac.in (G. Vijaya Prakash).

sources. The emission light was dispersed into a monochromator (Acton SP2300) coupled to a photo multiplier tube (PMT) through appropriate lens system. For time resolved emission, mechanical chopper (12 Hz), lock-in amplifier, and digital storage oscilloscope were employed to record the transient response.

3. Results and discussions

3.1. X-ray diffraction

The room temperature XRD patterns of un-doped $KCaBO_3$ and $x.0$ wt.% Yb^{3+} ($x = 2$ and 16) doped $KCaBO_3$:Er^{3+} phosphors are shown in the Figure 1. Obtained d-values from powder XRD data have been compared to that of similar un-doped $LiBaBO_3$ (JCPDS 81-1808) [28] and indexed accordingly. The sharp and single peaks of the XRD pattern suggest the formation of single-phase polycrystalline and can be identified as monoclinic crystal structure of space group $P2_1/c$ (14). Recently series of alkali and alkaline earth metal mixed borates have been investigated and produced large family of materials with different crystalline phases [24–26,28,29]. However the present study confirms that the synthesized material is single-phased $KCaBO_3$. Moreover, the observation of enhanced XRD peaks (ex: (1 1 2), (2 1 0)) without any peak shift appeared upon Er^{3+}/Yb^{3+} doping, indicating no significant changes in the host crystal structure with the doping. Table 1 further suggesting that the doping indeed facilitates the better crystallinity with interstitial incorporation and possibility of heterogeneous nucleation. The grain sizes estimated from the well-known Scherrer equation are in the range of 50–75 nm.

3.2. Downconversion emission under 532 nm excitation

The visible emission of $KCaBO_3$:Er^{3+} co-doped with various Yb^{3+} concentrations on excited with 532 nm laser is shown in Figure 2A. The spectra shows strong emission at around 547 nm with two low intense emissions at 830 and 980 nm, attributed to the Er^{3+} ion transitions $^4S_{3/2}$, $^4I_{9/2}$ and $^4I_{11/2}$ to the ground state $^4I_{15/2}$, respec-

Table 1
Estimated lattice parameters of un-doped $KCaBO_3$ and $x.0$ wt.% Yb^{3+} ($x = 2$ and 16)-doped $KCaBO_3$:Er^{3+}powders.

Compound	a (Å)	b (Å)	c (Å)	α	β	γ
$KCaBO_3$	11.46	6.90	7.25	90°	117.51°	90°
$KCaBO_3$:2 wt.%Er^{3+}-2 wt.% Yb^{3+}	11.97	6.95	7.09	90°	117.90°	90°
$KCaBO_3$:2wt.%Er^{3+}-16wt.% Yb^{3+}	11.75	6.90	7.05	90°	118.51°	90°

tively. Here, Er^{3+} ions are directly excited to $^2H_{11/2}$ and major parts of them deactivates to the ground state by emitting green light, along with other possible channels of radiative and non radiative decays (schematically shown in Figure 2B). Such downconversion (DC) emission intensities found same for all samples, irrespective of Yb^{3+} sensitizer concentration (Figure 2A).

3.3. Upconversion emission under 980 nm excitation

Upconversion (UC) is a sequential absorption of two infrared photons by rare earth ion low-energy, followed by the emission of visible photons from high-energy levels. The upconversion emission spectra of various Yb^{3+}-doped $KCaBO_3$:Er^{3+}phosphors, excited with 980 nm laser, has been recorded in the spectral region of 300–800 nm and shown in Figure 3. The upconversion emission spectra is dominated by the strong green emission of Er^{3+}, which is even visible to the naked eye (digital image are depicted as inset in Figure 3), at 524 and 545 nm are from transitions $^2H_{11/2}$, $^4S_{3/2}$ to the ground state $^4I_{15/2}$ of Er^{3+}, respectively. Other emission bands at around 487, 656 and 830 nm are corresponding to the transitions $^4F_{7/2}$, $^4F_{9/2}$ and $^4I_{9/2}$ to $^4I_{15/2}$ of Er^{3+}, respectively. However, the $KCaBO_3$:Er^{3+} powders with $Yb^{3+} = 0$ shows a faint emission at 830 nm ($^4I_{9/2} \rightarrow {}^4I_{15/2}$). This might be due to weak absorption cross-section of $^4I_{13/2}$ transition and large phonon energy of $KCaBO_3$ host [30], which could result into a quick multi-phonon relaxation between the energy levels of Er^{3+} ion (Figure 2B). Moreover as Yb^{3+} ion concentration is increasing, the green emission ($^2H_{11/2}$,$^4S_{3/2} \rightarrow {}^4I_{15/2}$) of Er^{3+} increasing monotonically, suggesting the important
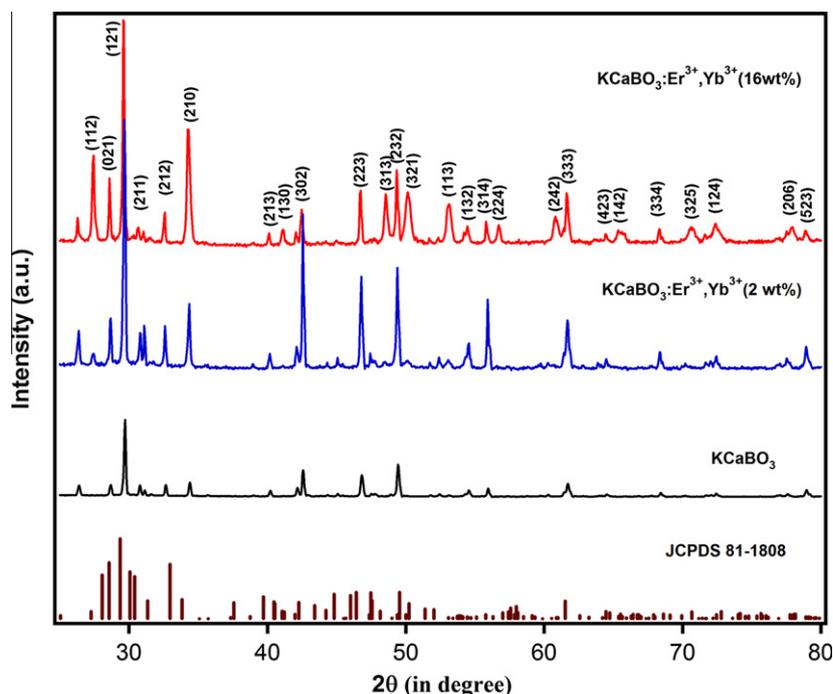

Figure 1. XRD pattern of un-doped $KCaBO_3$ and $x.0$ wt.% Yb^{3+} ($x = 2$ and 16) co-doped $KCaBO_3$:Er^{3+} at room temperature. Standard data of $LiBaBO_3$ (JCPDS 81-1808) is also given for comparison.
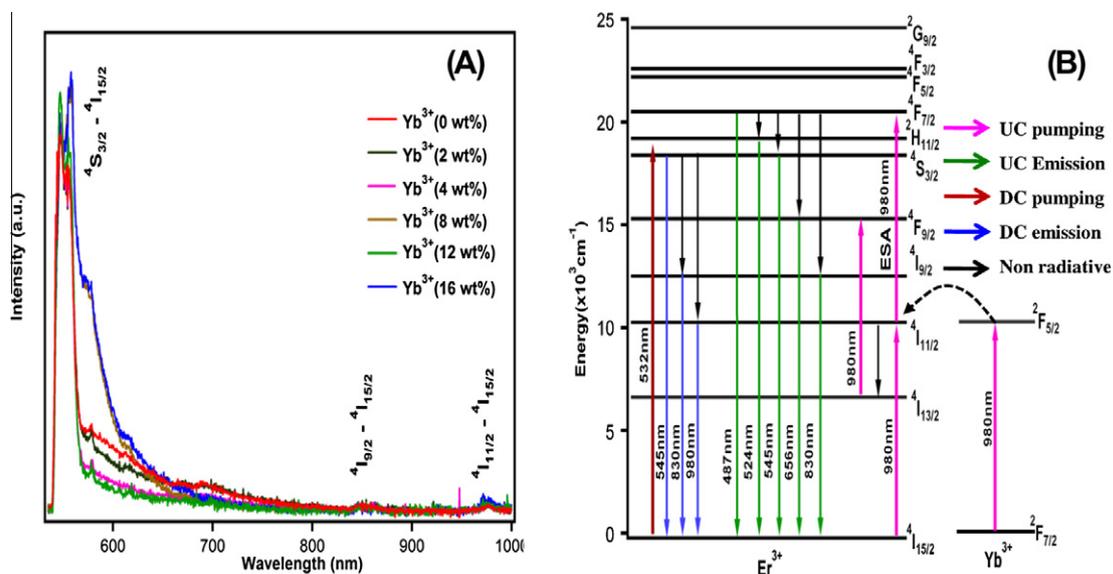
Figure 2. (A) Represents the DC emission of $x.0$ wt.% Yb^{3+} (x = 0, 2, 4, 8, 12 and 16) co-doped $KCaBO_3$:Er^{3+} phosphors at room temperature. λ_{ex} = 532 nm. (B) The schematic energy levels of Er^{3+} and Yr^{3+} ions containing UC and DC excitation and emission schemes.
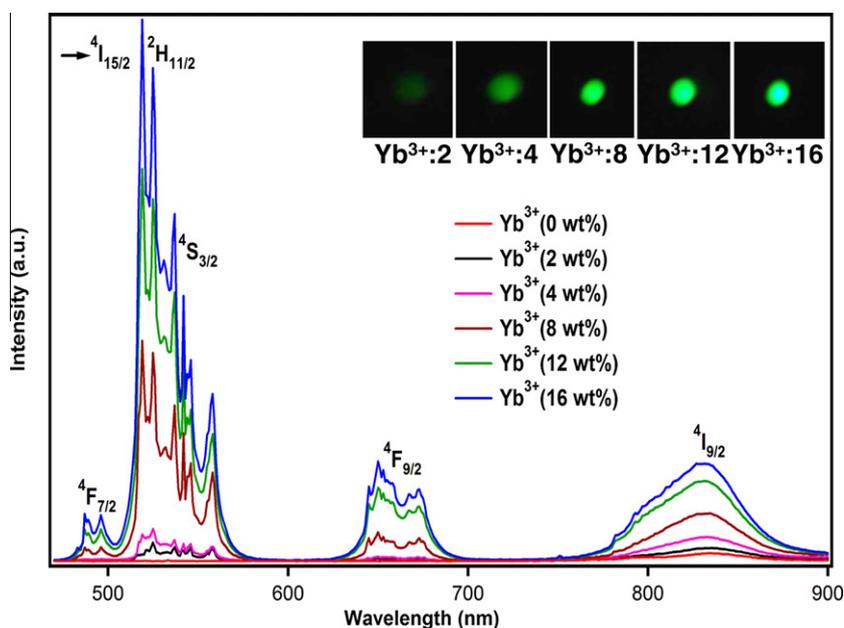

Figure 3. UC emission of $KCaBO_3$:Er^{3+} phosphors doped with different $x.0$ wt.% co-doping of Yb^{3+} (x = 0, 2, 4, 8, 12 and 16) at room temperature. λ_{ex} = 980 nm.

role of the energy transfer process between sensitizer (Yb^{3+}) to the active (Er^{3+}) rare-earth ion. Essentially the Yb^{3+} ion is used as sensitizer since it has a very high absorption energy level ($^2F_{5/2} \rightarrow {}^2F_{7/2}$) at excitation wavelength. Therefore upon excitation with 980 nm, apart from excited state absorption (ESA), an efficient energy transfer (ET) from Yb^{3+} to Er^{3+} is possible due to spectral overlap between Yb^{3+} transition of $^2F_{5/2} \rightarrow {}^2F_{7/2}$ and that of Er^{3+} absorption energy $^4I_{11/2} \rightarrow {}^4I_{15/2}$, which significantly improves the UC emission process (schematic Figure 2B).

The enhancement in the upconverted emission intensities as a function of Yb^{3+} concentration can be explained on the basis of modification of inter ionic distance between the Er^{3+} and Yb^{3+} ions. With the increase of Yb^{3+} ion concentration, the average distance between the Er^{3+} and Yb^{3+} ions decreases, which automatically

Table 2

The UC and DC emission lifetimes and Green-to-Red (G/R) integrated UC emission ratios of $KCaBO_3$:Er^{3+} phosphors co-doped with $x.0$ wt.% Yb^{3+} (x = 2, 4, 8, 12 and 16). Parenthesis values of 524 nm UC emission indicate the relative integrated areas of fast and slow components.

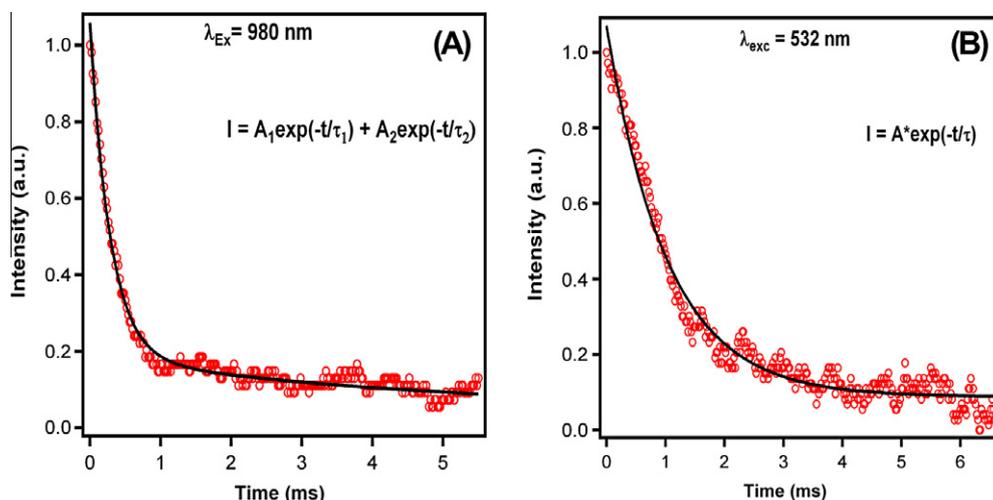| Yb^{3+} ion concentration (wt.%)	G/R ratio	524 nm UC emission (λ_{exc} = 980 nm) ($^2H_{11/2}$, $^4S_{3/2}$ $\rightarrow {}^4I_{15/2}$ of Er^{3+})		547 nm DC emission (λ_{exc} = 532 nm) ($^4S_{3/2} \rightarrow {}^4I_{15/2}$ of Er^{3+})
x=		τ_1(ms)	τ_2(ms)	τ(ms)
2	4.7	0.69(48.00%)	0.61(52.00%)	1.00
4	5.6	2.20(34.70%)	0.22(65.30%)	0.85
8	6.4	2.30(5.78%)	0.27(94.22%)	0.86
12	6.6	2.20(9.72%)	0.29(90.27%)	0.92
16	7.7	4.60(14.15%)	0.29(85.84%)	0.95

Figure 4. The emission decay curves of (A) UC emission of 524 nm ($^2H_{11/2}$, $^4S_{3/2}$ → $^4I_{15/2}$ of Er^{3+}) and (B) DC emission of 547 nm ($^4S_{3/2}$ → $^4I_{15/2}$ of Er^{3+}) of 16 wt.% Yb^{3+} co-doped $KCaBO_3$:Er^{3+} phosphor. For UC and DC emission the excitation wavelengths are 980 and 532 nm, respectively.

enhance the energy transfer process from Yb^{3+} to Er^{3+} ions. Such energy transfer increases the high energy excited-state populations of the Er^{3+} ions, leading to increase in the blue, green, red and near-infrared emission intensities. Most importantly, it is seen from the Figure 3, the intensity of the green emission increases dramatically with the Yb^{3+}-concentration compared to that of the other red (656 nm) and near-infrared (830 nm) emissions. This is possibly due to the probability of electron in the $^4I_{11/2}$ state gets promoted to the $^4F_{7/2}$ states via an energy-transfer upconversion process, which is much higher than that of nonradiative relaxation to the $^4I_{13/2}$ (for 656 nm emission) and $^4I_{9/2}$ (for 830 nm emission) states. Also the change the crystal field symmetry around rare earth ion and crystallinity may also influence emission intensities and broadness. The integrated UC emission intensities ratios of green ($^2H_{11/2}$,$^4S_{3/2}$ → $^4I_{15/2}$) and red ($^4F_{9/2}$ → $^4I_{15/2}$) transitions for varied Yb^{3+}-concentrations in $KCaBO_3$:Er^{3+} are given in Table 2. The monotonic increase in the G/R intensity ratio indicating the good crystallinity of the host, which is also evident from XRD analysis (Figure 1). Further, the increase in the inhomogeneous broadening (the width of UC emission lines) with the increase of Yb^{3+} concentrations can be attributed to the change in the ligand field around Er^{3+} ions [31]. When the trivalent ions (Re^{3+}) are to be incorporated into the host matrix of divalent (such as Ca^{2+}) ions, the charge compensation is necessarily required. The studies of different charge compensation models on the luminescent properties of rare-earth (Re^{3+}) ions were reported for different hosts in the recent past [32–35]. In the present system, the charge compensation is possible from two mechanisms: (i) $2Ca^{2+} = Re^{3+} + K^+$ or (ii) $3Ca^{2+} = 2Re^{3+} +$ interstitial vacancies [35]. Based on the observation of enhanced luminescence properties and improved crystallinity, the rare earth ions in the host $KCaBO_3$ possibly occupy the charge compensated sites of Ca^{2+} ions by the dominant mechanism of $2Ca^{2+} = Re^{3+} + K^+$.

Finally the radiative decay times, defined as the time required for the luminescence intensity to decrease to $1/e$ of its initial value, is also calculated for the most intense UC emission (524 nm, $^2H_{11/2}$ → $^4I_{15/2}$) and DC emission (547 nm, $^4S_{3/2}$ → $^4I_{15/2}$) of Er^{3+} ion. Example decay curves are given in Figure 4 and corresponding lifetimes were tabulated in Table 2. Interestingly, the DC emission resulted into a single exponential whereas UC emission decay resulted as double exponential in nature. Without any interaction between emitting rare-earth ions, the decay can be fitted to a single exponential [36]. However, when ion-ion interactions and energy transfer are predominant, the resultant emission could deviate from single exponential and can have both fast and slow components. On comparison, the UC green emission decay is predominantly faster ($\sim$0.2 ms) compared to that of DC green emission ($\sim$0.9 ms) and both decays are more or less invariant with the Yb^{3+} sensitizer co-doping.

4. Conclusions

Single phase monoclinic $KCaBO_3$:Er^{3+} phosphors with varied Yb^{3+} concentrations were synthesized by solid state diffusion technique at 950 °C and their upconversion under near-infrared excitation are reported for the first time. The UC spectra of all co-doped samples showed strong green emission of Er^{3+}, even visible to naked eye, attributed to the transitions $^2H_{11/2}$, $^4S_{3/2}$ to ground state of $^4I_{15/2}$. The increase in the green emission intensities as a function of sensitizer (Yb^{3+}) concentration is explained based on modification of inter ionic distance, two photon absorption and efficient energy transfer between the Er^{3+} and Yb^{3+} ions. The monotonic increase in the green-to-red intensity ratio suggesting the increased effects of good crystallinity, which was also supported by X-ray diffraction analysis. Enhanced green emission from these mixed borate phosphors could be found very useful for upconversion phosphors.

Acknowledgements

References

[1] T. Sandrock, H. Scheife, E. Heumann, G. Huber, Opt. Lett. 22 (1997) 1185.
[2] E. Dowing, L. Hesselink, J. Ralston, R. Macfarlane, Science 273 (1996) 1185.
[3] S.Q. Xu, H.P. Ma, D.W. Fang, Z.X. Zhang, Z.H. Jiang, Mater. Lett. 59 (2005) 3066.
[4] C.G. Morgan, S. Dad, A.C. Mitchell, J. Alloys Compd. 451 (2008) 526.
[5] N. Tyagi, A. Amarnath Reddy, R. Nagarajan, Opt. Mater. 33 (2010) 42.
[6] D. Dosev, I.M. Kennedy, M. Godlewski, I. Gryczynski, K. Tomsia, E.M. Goldys, Appl. Phys. Lett. 88 (2006) 011906.
[7] H. Lin, G. Meredith, S. Jiang, X. Peng, T. Luo, N. Peyghambarian, E. Yue-Bun Pun, J. Appl. Phys. 93 (2003) 186.
[8] R.H. Page, K.I. Schaffers, P.A. Waide, J.B. Tassano, S.A. Payne, W.F. Krupke, W.K. Bischel, J. Opt. Soc. Am. B 15 (1998) 996.
[9] N. Menyuk, K. Dwight, J.W. Pierce, Appl. Phys. Lett. 21 (1972) 159.
[10] G. Blasse, B.C. Grabmaier, Luminescent Materials, Springer Verlag, Berlin, 1994. p. 195.

[11] F. Auzel, in: B. Di Bartolo (Ed.), Spectroscopy and Dynamics of Collective Excitations in Solids, Plenum, New York, 1997, p. 537.

[12] M. Malinowski, Z. Frukacz, M.F. Joubert, B. Jacquier, J. Lumin. 75 (1997) 333.

[13] I.R. Martin, V.D. Rodriguez, V. Lavin, U.R. Rodriguez-Mendoza, J. Lumin. 72–74 (1997) 954.

[14] B. Simondi-Teisseire, B. Viana, D. Vivien, A.M. Lejus, Opt. Mater. 6 (1996) 267.

[15] J.A. Hutchinson, H.R. Verdun, B.H.T. Chai, L.D. Merkle, Opt. Mater. 3 (1994) 287.

[16] E. Cantelar, F. Cusso, Appl. Phys. B: Lasers Opt. 69 (1999) 29.

[17] L. Wang, X. Xue, H. Chen, D. Zhao, W. Qin, Chem. Phys. Lett. 485 (2010) 183.

[18] H.S. Biao Dong et al., J. Phys. Chem. C 112 (2008) 1435.

[19] A. Patra, P. Ghosh, P.S. Chowdhury, M. Alencar, B.W. Lozano, N. Rakov, G.S. Maciel, J. Phys. Chem. B 109 (2005) 10142.

[20] C.H. Liu, D.P. Chen, J. Mater. Chem. 17 (2007) 3875.

[21] H.X. Mai, Y.W. Zhang, L.D. Sun, C.H. Yan, J. Phys. Chem. C 111 (2007) 13721.

[22] G.Y. Chen, Y. Liu, Z.G. Zhang, B. Aghahadi, G. Somesfalean, Q. Sun, F.P. Wang, Chem. Phys. Lett. 448 (2007) 127.

[23] G. Kaur, S.K. Singh, S.B. Rai, J. Appl. Phys. 107 (2010) 073514.

[24] P. Li, Z. Wang, Z. Yang, Q. Guo, G. Fu, X.Z. Li, Y.P. Xu, Mater. Res. Bull. 44 (2009) 2068.

[25] Z. Wang, Z. Yang, P. Li, Q. Guo, Y. Yang, J. Rare Earths 28 (2010) 30.

[26] L. Wu, X.L. Chen, H. Li, M. He, Y.P. Xu, X.Z. Li, Inorg. Chem. 44 (2005) 6409.

[27] A. Altomare et al., J. Appl. Cryst. 37 (2004) 1025.

[28] M. Schlaeger, R.Z. Hoppe, Anorg. Allg. Chem. 619 (1993) 976.

[29] L. Wu, Y. Zhang, Y.F. Kong, T.Q. Sun, J.J. Xu, X.L. Chen, Inorg. Chem. 46 (2007) 5207.

[30] Z. Shang, G. Ren, Q. Yang, C. Xu, Y. Liu, Y. Zhang, Q. Wu, J. Alloy. Comp. 460 (2007) 539.

[31] V.K. Komarala, Y. Wang, M. Xiao, Chem. Phys. Lett. 490 (2010) 189.

[32] P. Li, Z. Zhang, K. Zhang, Z. Yang, Z. Wang, Q. Guo, Chin. Phys. Lett. 6 (2008) 274.

[33] A. Xie, X. Yuan, F. Wang, Y. Shi, Z. Mu, J. Phys. D: Appl. Phys. 43 (2010) 055101.

[34] A.J. Lenus, M.T. Jose, M. Yousuf, K.G. Rajan, A.R. Lakshmanan, Radiat. Meas. 33 (2001) 397.

[35] J. Liu, H. Lian, C. Shi, Opt. Mater. 29 (2007) 1591.

[36] G. Lakshminarayana, H. Yang, J. Qiu, J. Solid State Chem. 182 (2009) 669.